Incorporation of bifunctional aminopyridine into a NbO-type MOF for markedly enhanced adsorption of C_2H_2 and CO_2 over CH_4

Minghui He, Tingting Xu, Zhenzhen Jiang, Luyao Yang, Ying Zou, Fengjie Xia, Xia Wang, Xiaojuan Wang* and Yabing He*

Key Laboratory of the Ministry of Education for Advanced Catalysis Materials, College of Chemistry and Life Sciences, Zhejiang Normal University, Jinhua 321004, China. E-mail: wangxj@zjnu.cn; heyabing@zjnu.cn

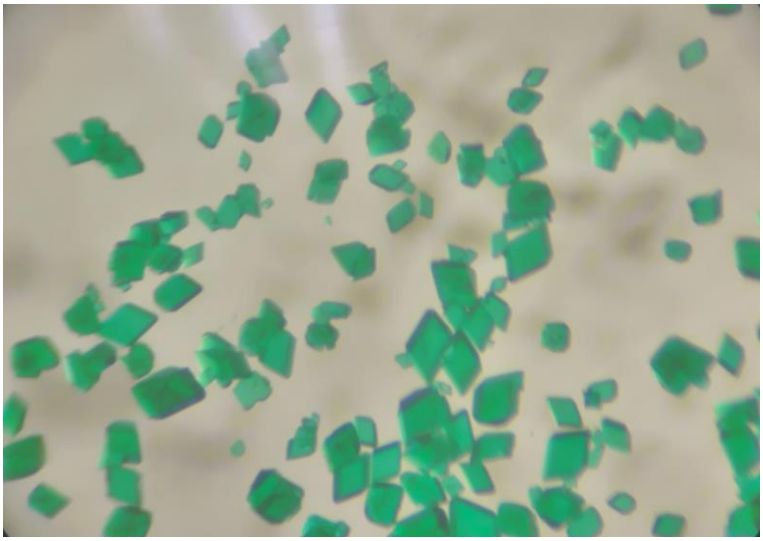

Fig. S1 The electronic photograph of the as-synthesized **ZJNU-98**.

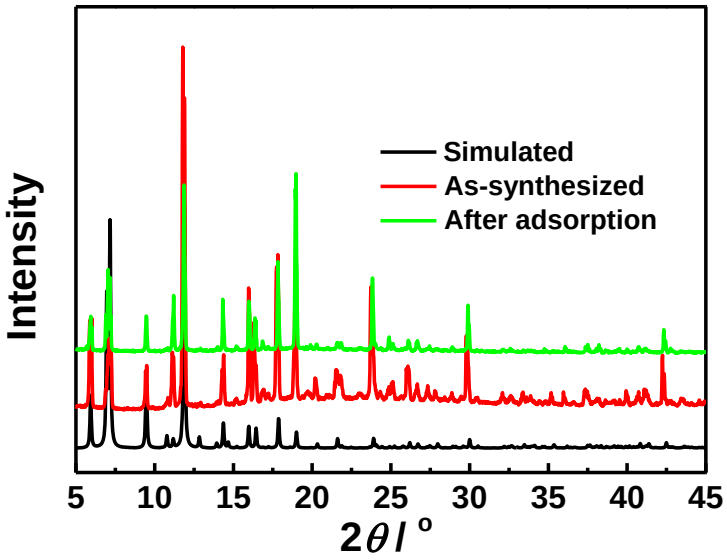

Fig. S2 Comparison of the experimental and simulated PXRD patterns of **ZJNU-98**.

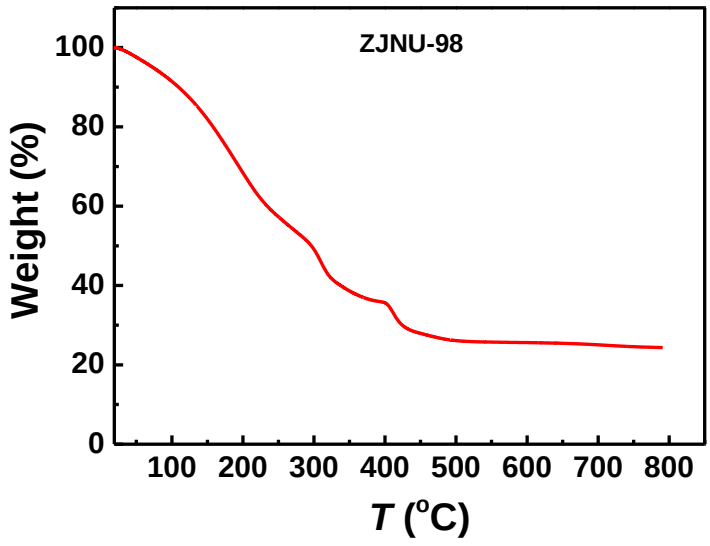

Fig. S3 TGA curve of the as-synthesized **ZJNU-98** under nitrogen atmosphere.

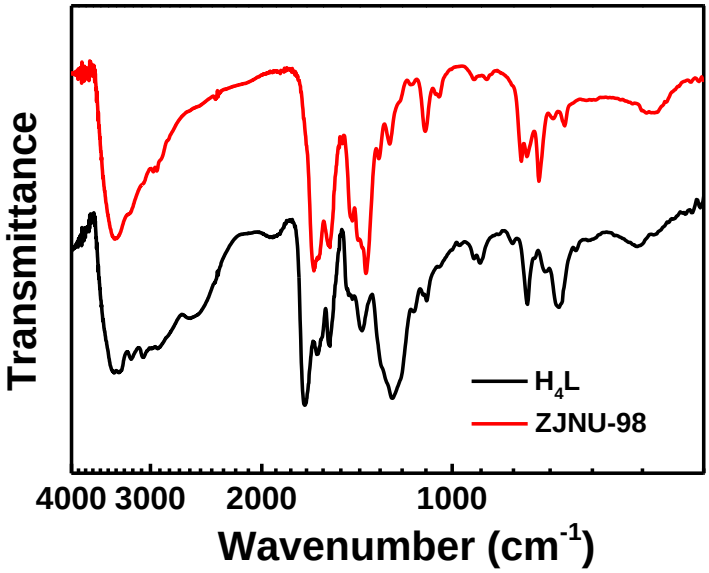

Fig. S4 Comparison of FTIR spectra of the ligand H_4L and its corresponding as-synthesized MOF **ZJNU-98**.

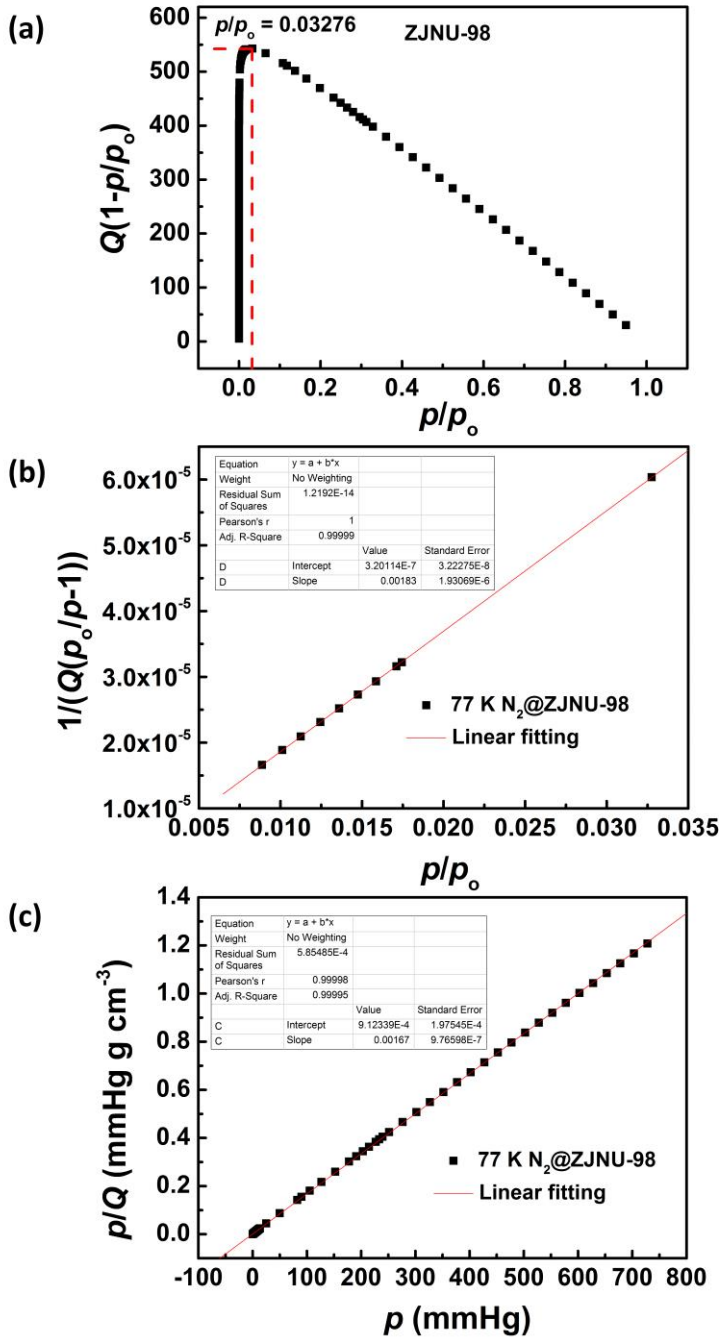

S_{BET} = 1/(3.20114×10^{-7}+ 0.00183)/22414 × 6.023 × 10^{23} × 0.162 × 10^{-18} = 2378 m^2 g^{-1}

$S_{Langmuir}$= (1/0.00167)/22414 × 6.023 × 10^{23} × 0.162 × 10^{-18} = 2607 m^2 g^{-1}

BET constant C = 1 + 0.00183/ 3.20114×10^{-7} = 5717

$$(P/P_o)_{n_m} = \frac{1}{\sqrt{C}+1} = 0.01305$$

Fig. S5 The consistency plot (a), BET surface area plot (b), and Langmuir surface area plot (c) for **ZJNU-98**.

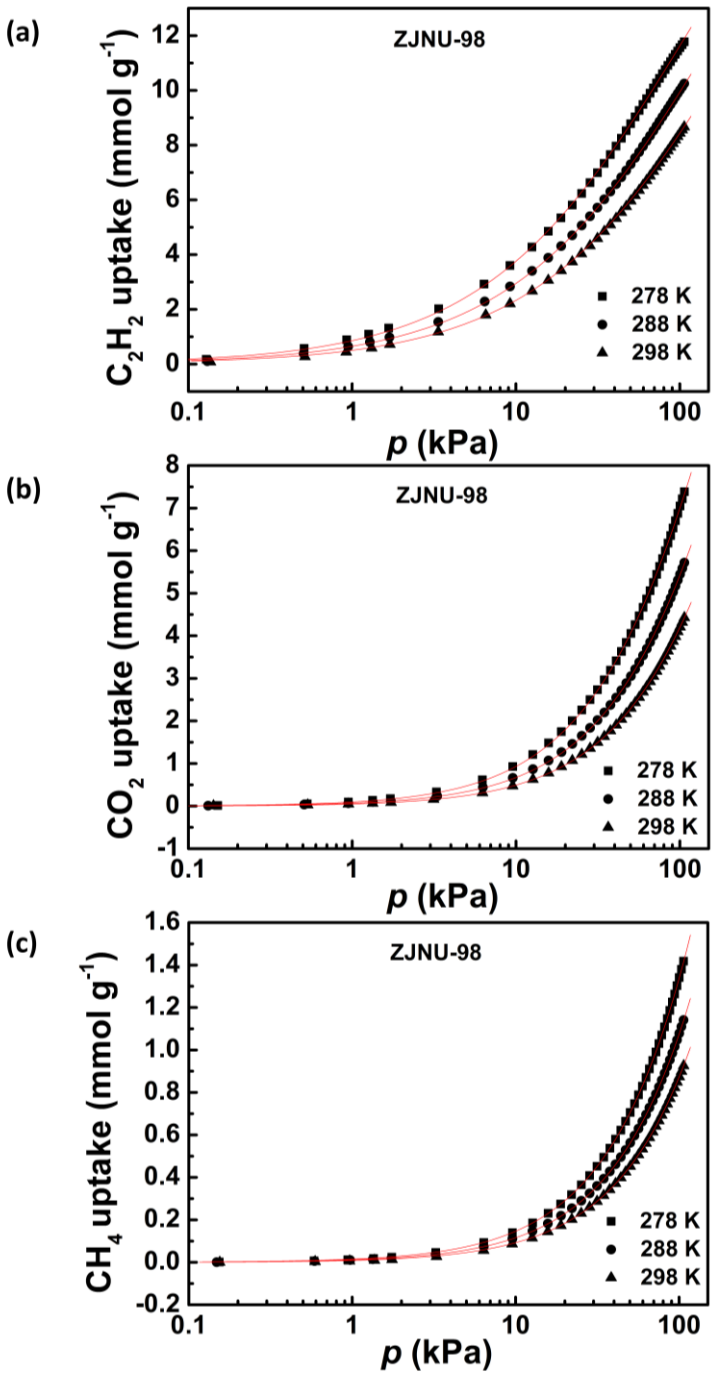

Fig. S6 Comparison of the pure-component isotherm data for (a) C_2H_2, (b) CO_2, and (c) CH_4 in **ZJNU-98** with the fitted isotherms at 278 K, 288 K, and 298 K.

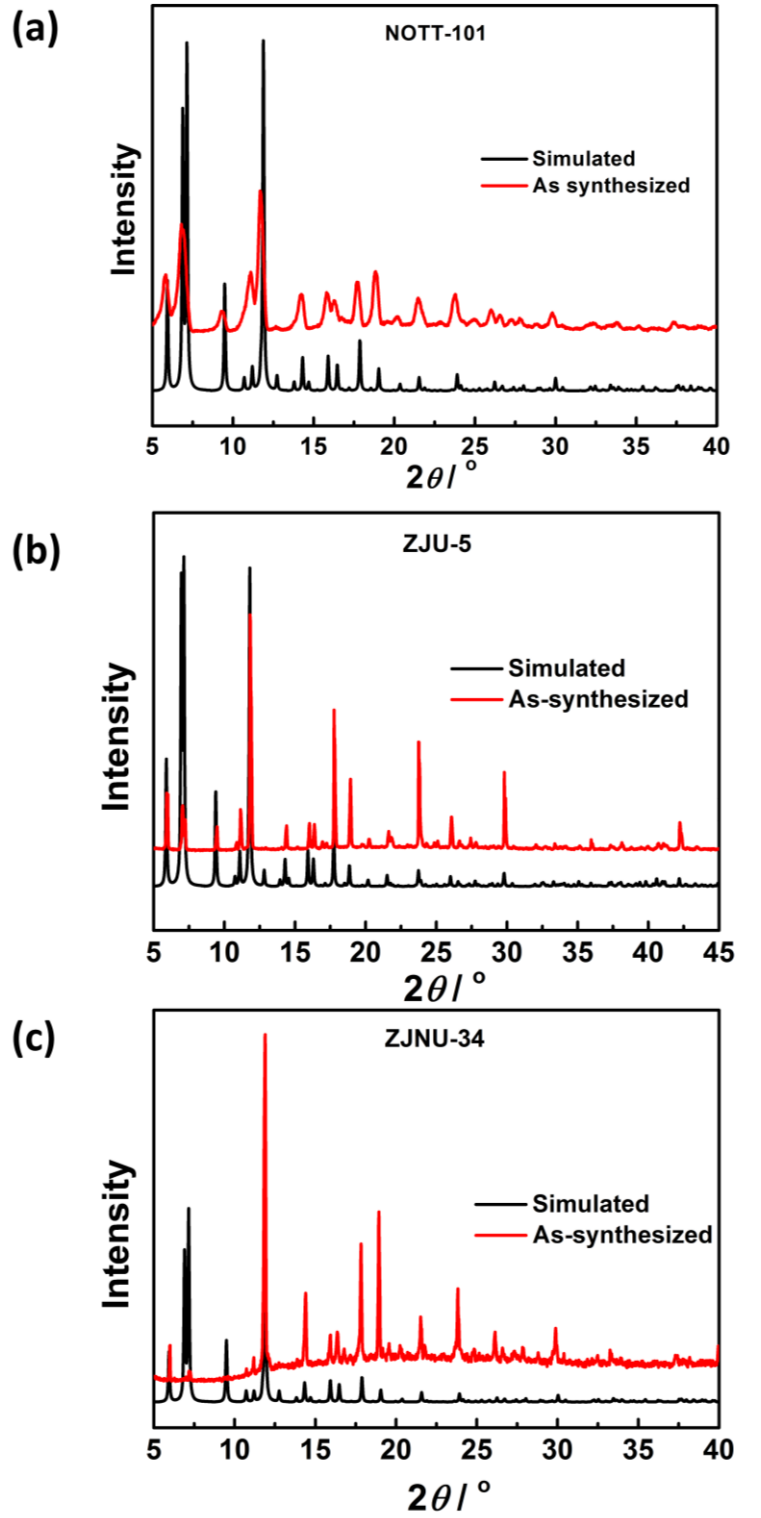

Fig. S7 Comparison of the experimental and simulated PXRD patterns of (a) NOTT-101, (b) ZJU-5, and (c) ZJNU-34.

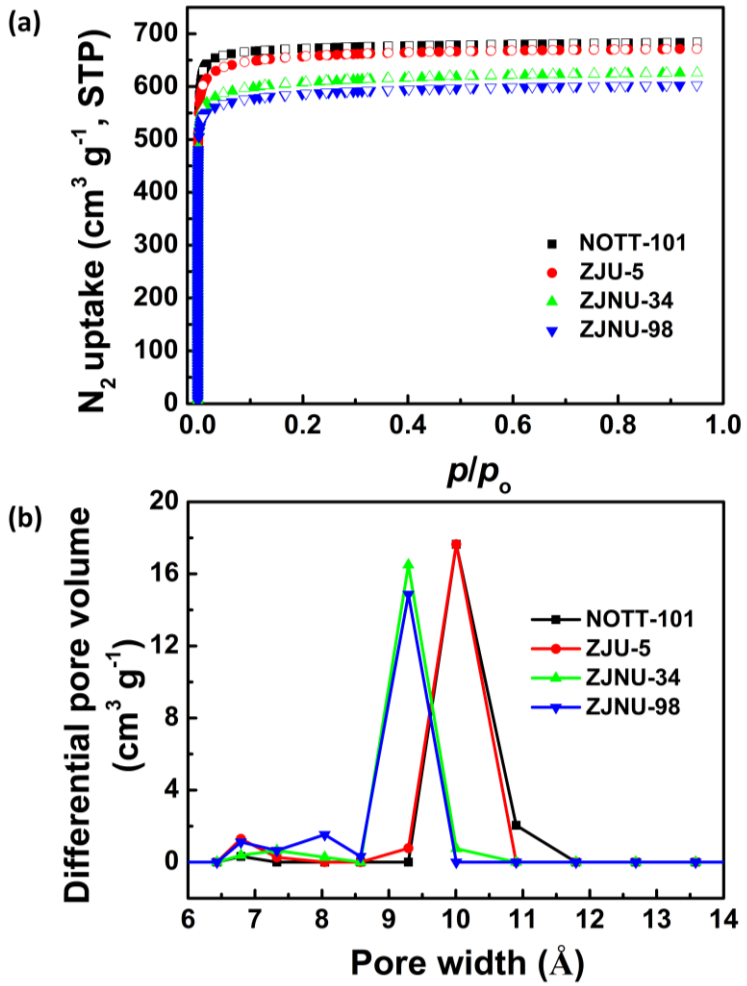

Fig. S8 Comparison of (a) N_2 isotherms at 77 K and (b) DFT-derived PSD of **ZJNU-98**, ZJNU-34, ZJU-5 and NOTT-101.

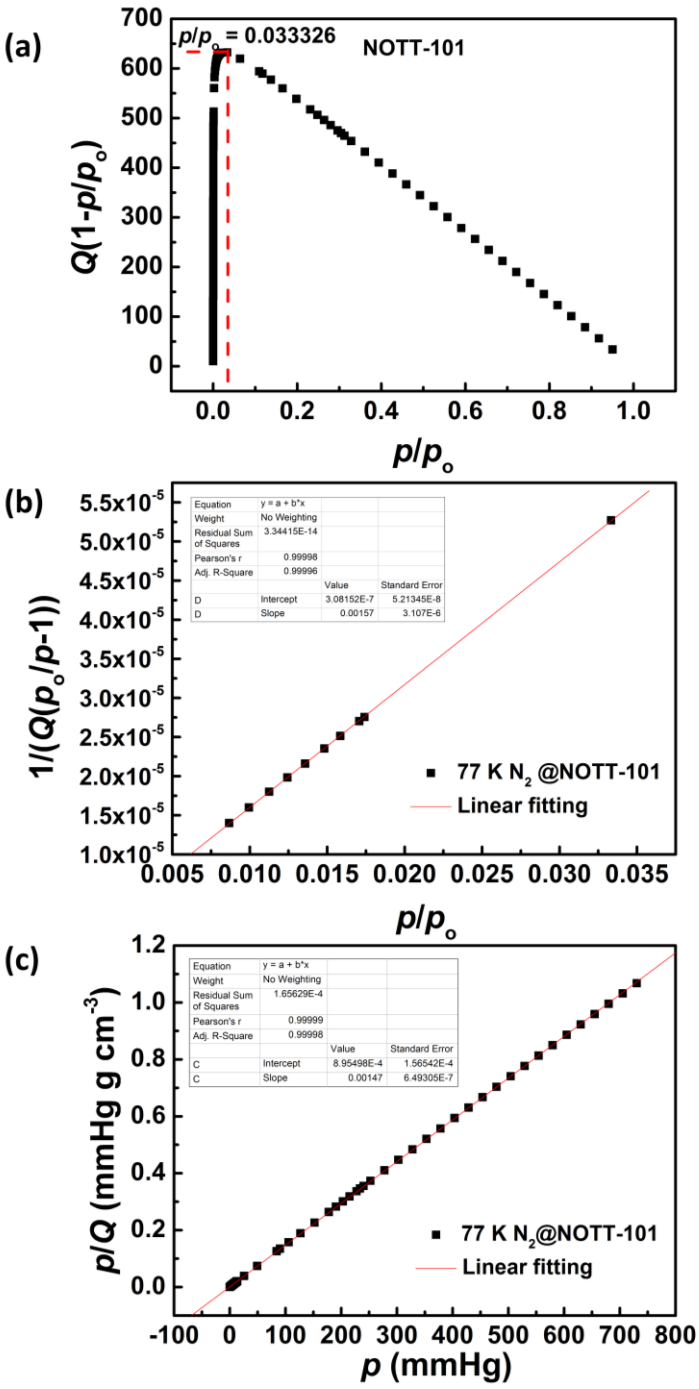

S_{BET} = 1/(3.08152 ×10^{-7}+ 0.00157)/22414 × 6.023 × 10^{23} × 0.162 × 10^{-18} = 2772 m^2 g^{-1}

$S_{Langmuir}$ = (1/0.00147)/22414 × 6.023 × 10^{23} × 0.162 × 10^{-18} = 2961 m^2 g^{-1}

BET constant C = 1 + 0.00157/3.08152 ×10^{-7} = 5096

$$(P/P_o)_{n_m} = \frac{1}{\sqrt{C}+1} = 0.01381$$

Fig. S9 The consistency plot (a), BET surface area plot (b), and Langmuir surface area plot (c) for **NOTT-101**.

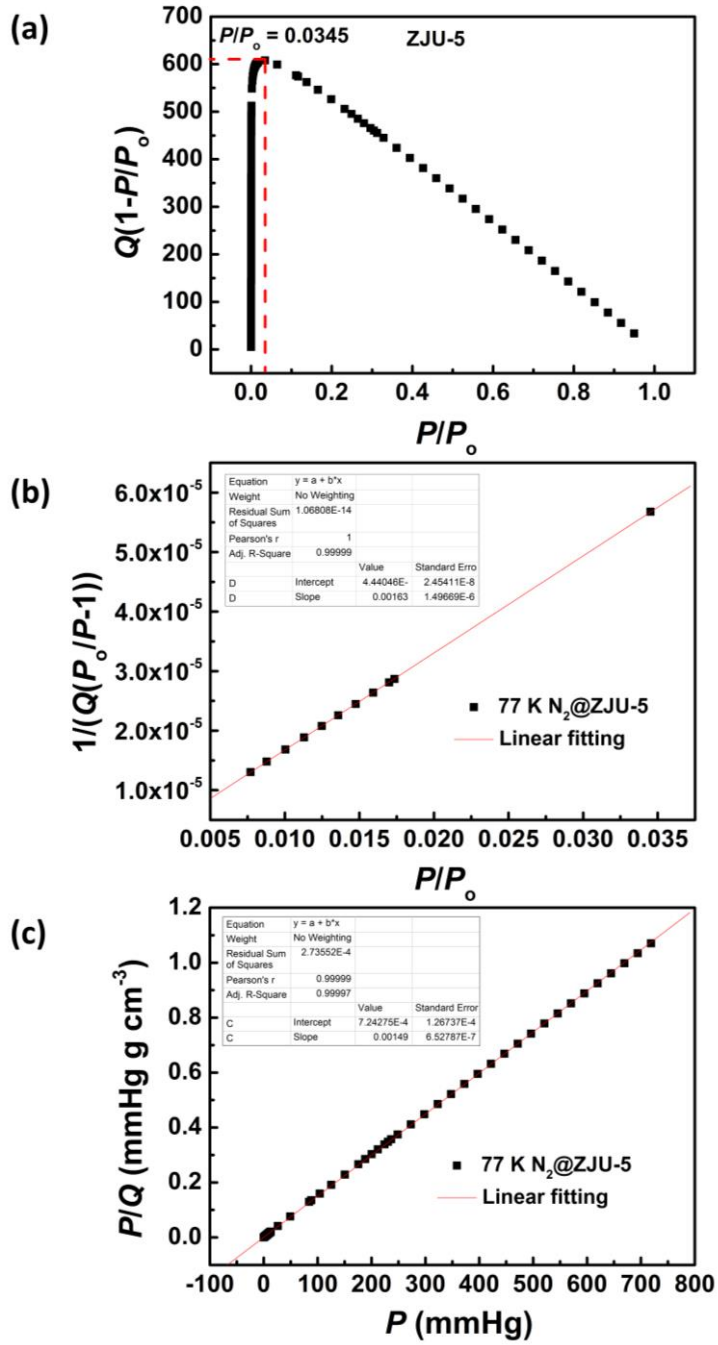

S_{BET} = 1/(4.44046×10^{-7}+ 0.00163)/22414 ×6.023 ×10^{23} ×0.162 ×10^{-18} = 2670 m^2 g^{-1}

$S_{Langmuir}$ = (1/0.00149)/22414 ×6.023 ×10^{23} ×0.162 ×10^{-18} = 2922 m^2 g^{-1}

BET constant C = 1 + 0.00163/4.44046×10^{-7} = 3672

$$(p/p_o)_{n_m} = \frac{1}{\sqrt{C}+1} = 0.016235$$

Fig. S10 The consistency plot (a), BET surface area plot (b), and Langmuir surface area plot (c) for **ZJU-5**.

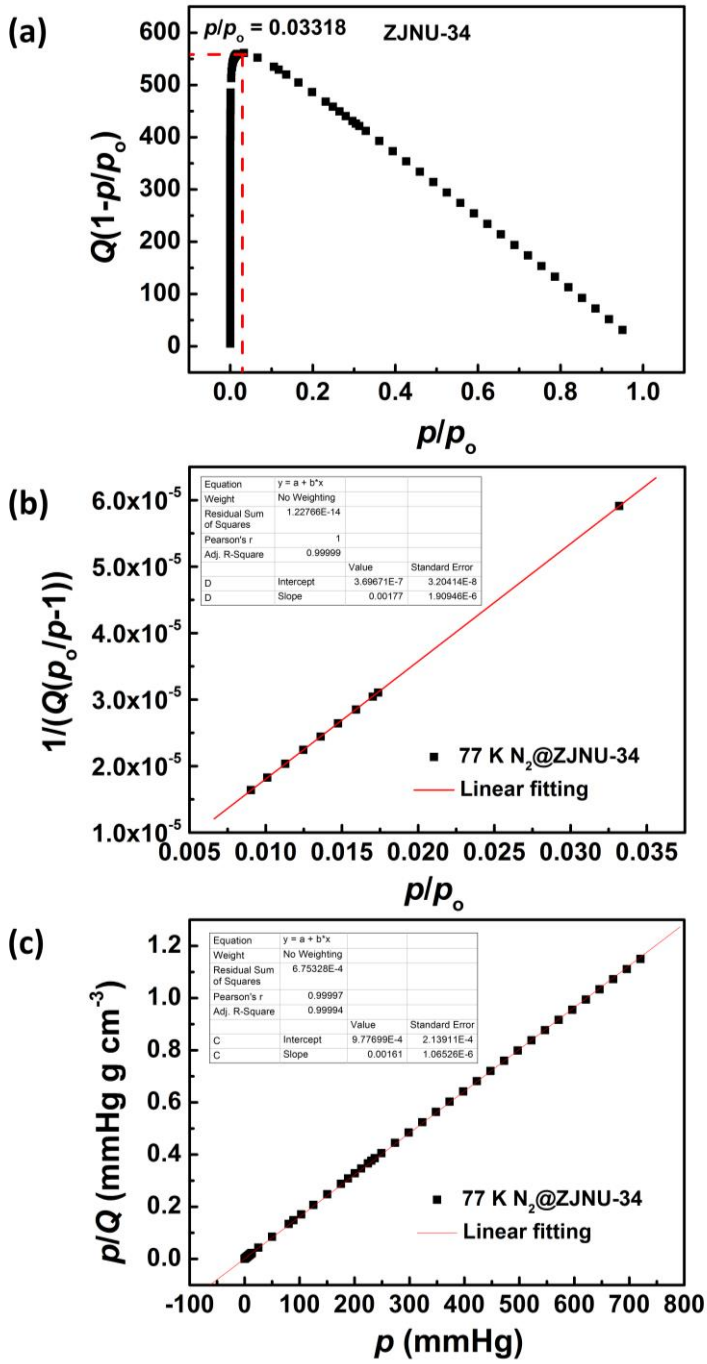

S_{BET} = 1/(3.69671 ×10^{-7}+ 0.00177)/22414 × 6.023 × 10^{23} × 0.162 × 10^{-18} = 2459 m^2 g^{-1}

$S_{Langmuir}$ = (1/0.00161)/22414 × 6.023 × 10^{23} × 0.162 × 10^{-18} = 2704 m^2 g^{-1}

BET constant C = 1 + 0.00177/3.69671 ×10^{-7} = 4789

$$(p/p_o)_{n_m} = \frac{1}{\sqrt{C}+1} = 0.01424$$

Fig. S11 The consistency plot (a), BET surface area plot (b), and Langmuir surface area plot (c) for **ZJNU-34**.

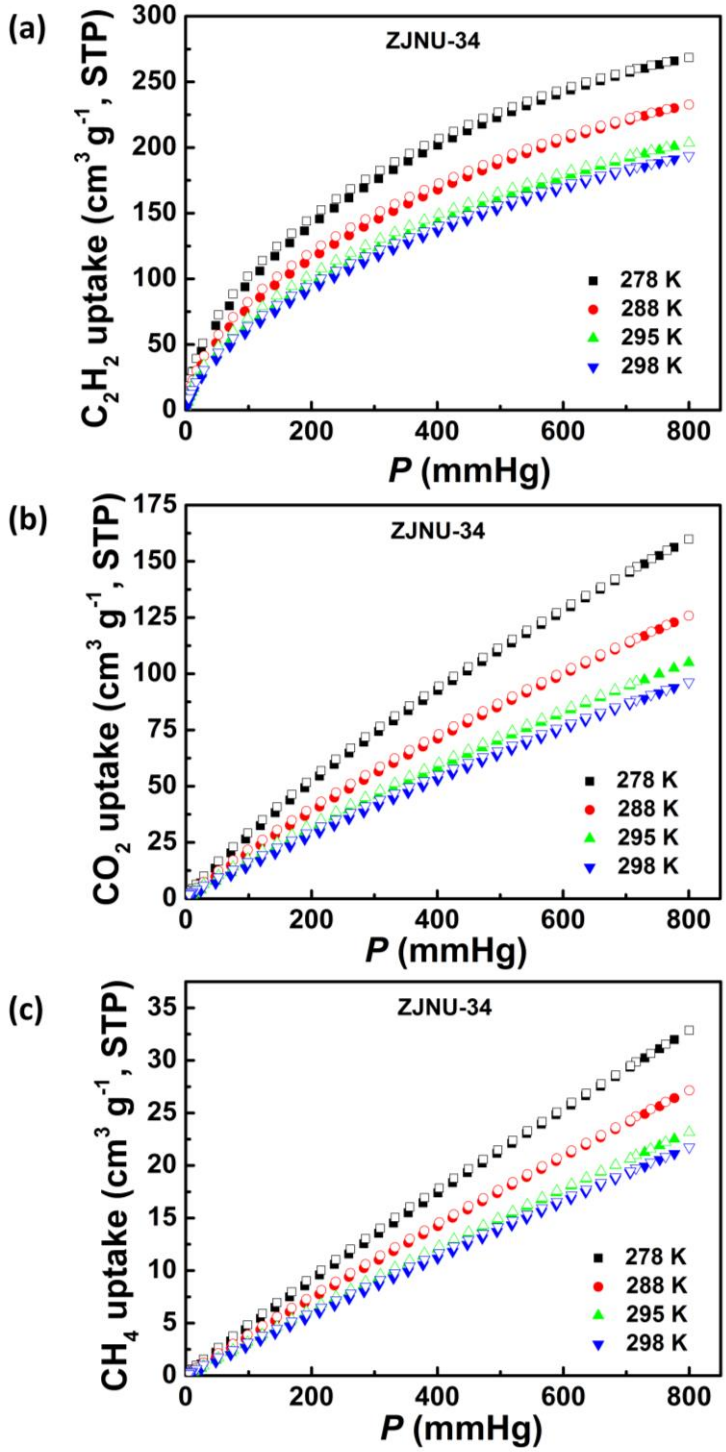

Fig. S12 (a) C_2H_2, (b) CO_2, and (c) CH_4 adsorption-desorption isotherms of **ZJNU-34** at four different temperatures of 298 K, 295 K, 288 K, and 278 K. The solid and open symbols represent adsorption and desorption, respectively.

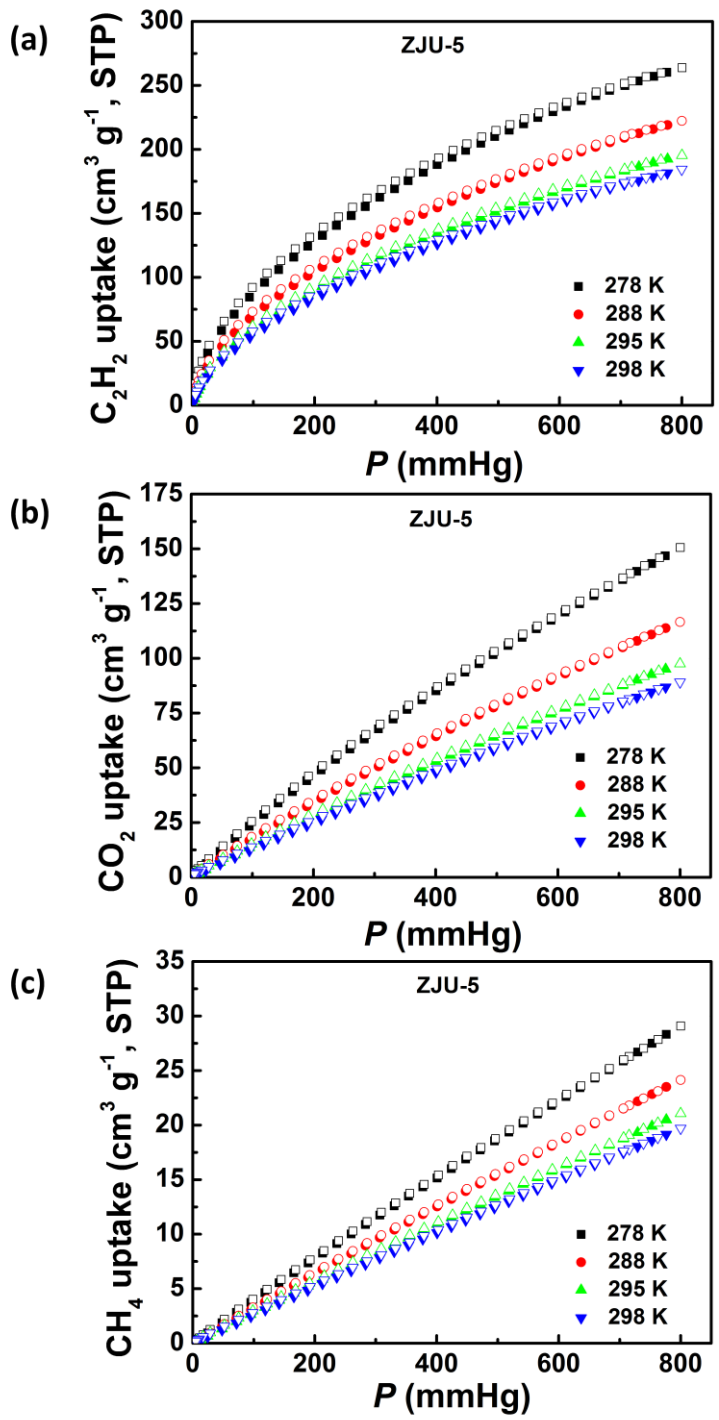

Fig. S13 (a) C_2H_2, (b) CO_2, and (c) CH_4 adsorption-desorption isotherms of **ZJU-5** at four different temperatures of 298 K, 295 K, 288 K, and 278 K. The solid and open symbols represent adsorption and desorption, respectively.

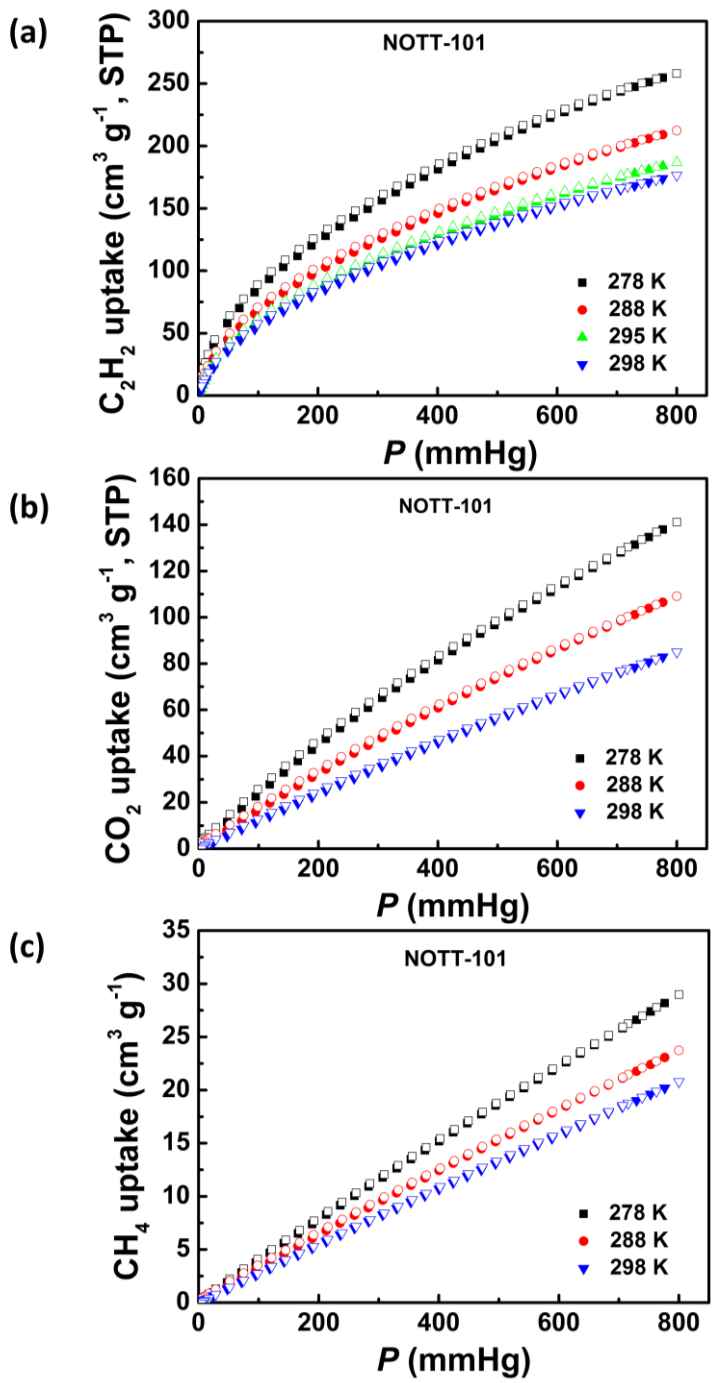

Fig. S14 (a) C_2H_2, (b) CO_2, and (c) CH_4 adsorption-desorption isotherms of **NOTT-101** at four different temperatures of 298 K, 295 K, 288 K, and 278 K. The solid and open symbols represent adsorption and desorption, respectively.

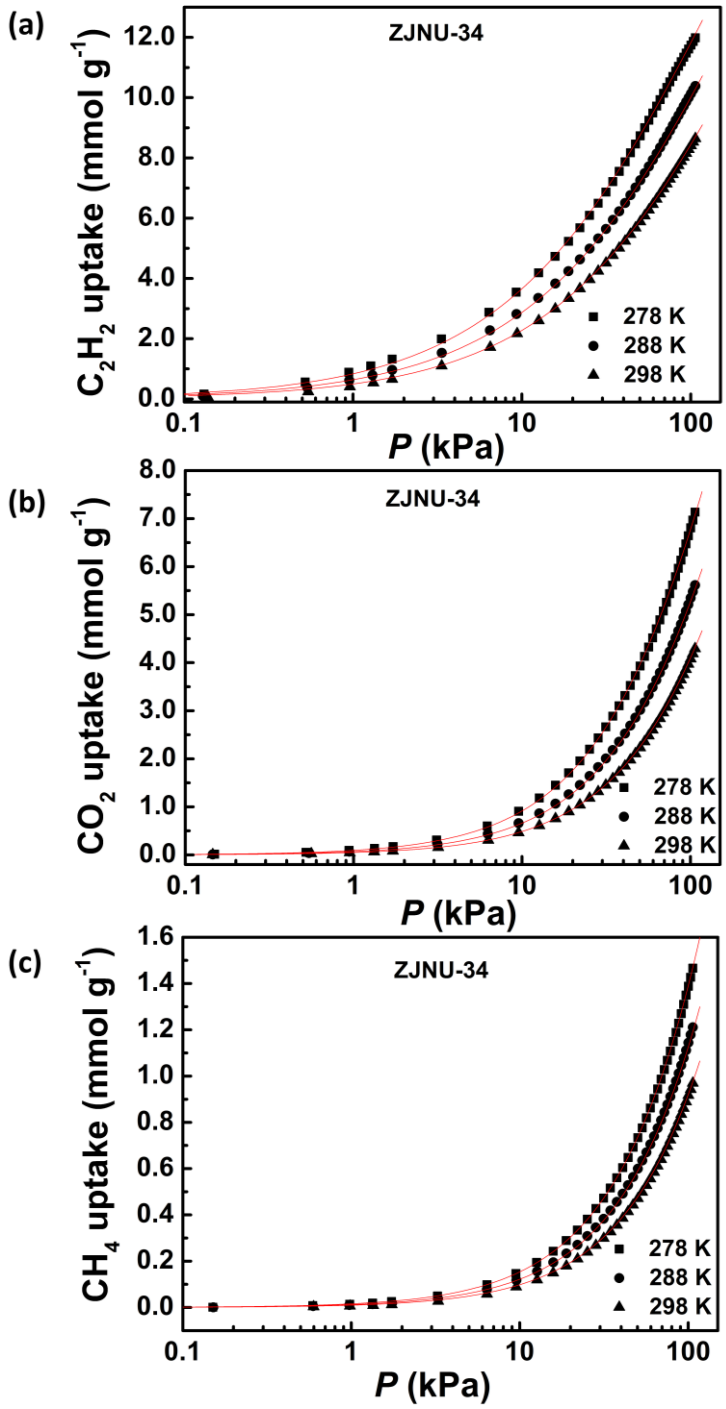

Fig. S15 Comparison of the pure-component isotherm data for (a) C_2H_2, (b) CO_2, and (c) CH_4 in **ZJNU-34** with the fitted isotherms at 278 K, 288 K, and 298 K.

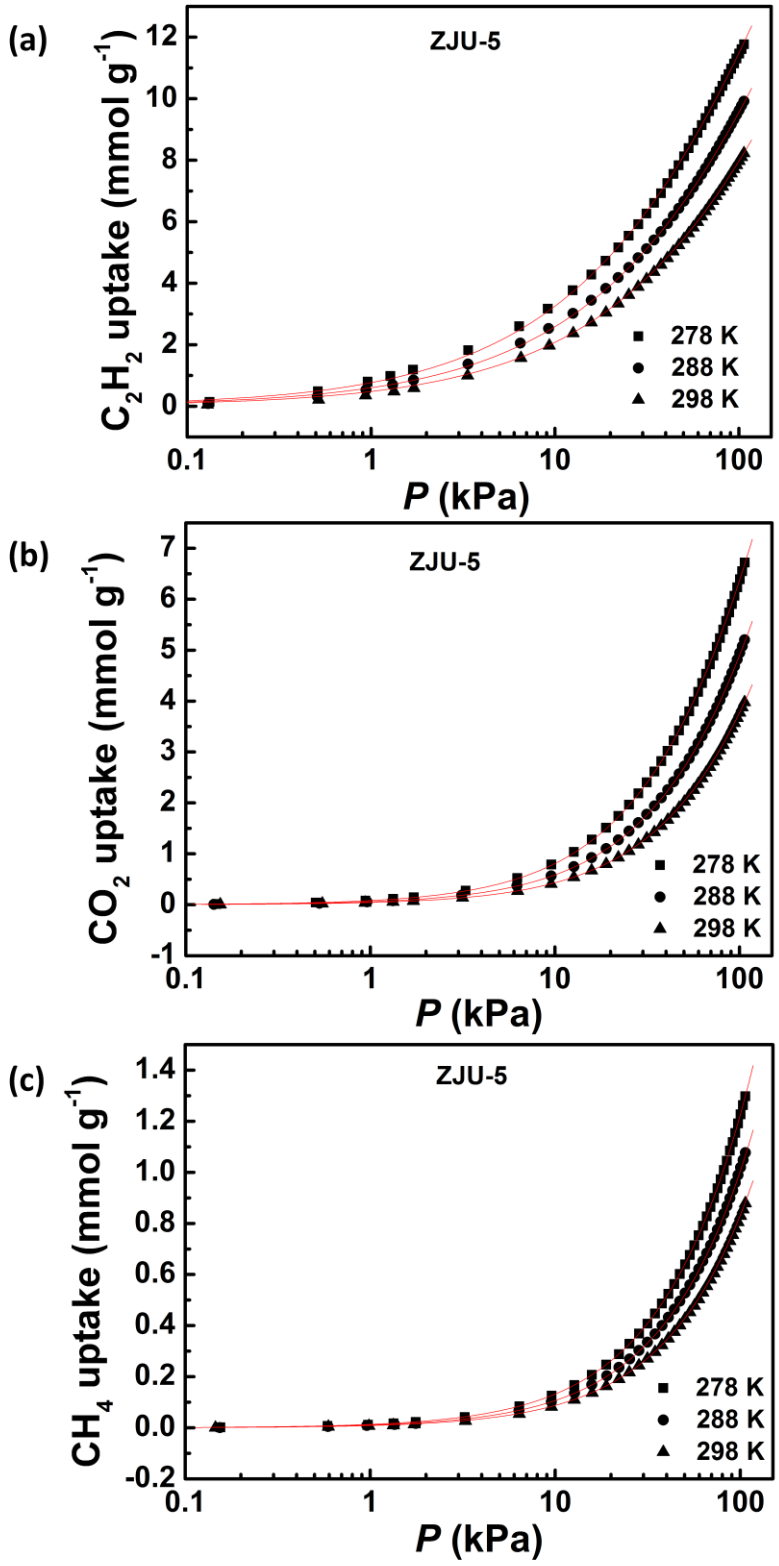

Fig. S16 Comparison of the pure-component isotherm data for (a) C_2H_2, (b) CO_2, and (c) CH_4 in **ZJU-5** with the fitted isotherms at 278 K, 288 K, and 298 K.

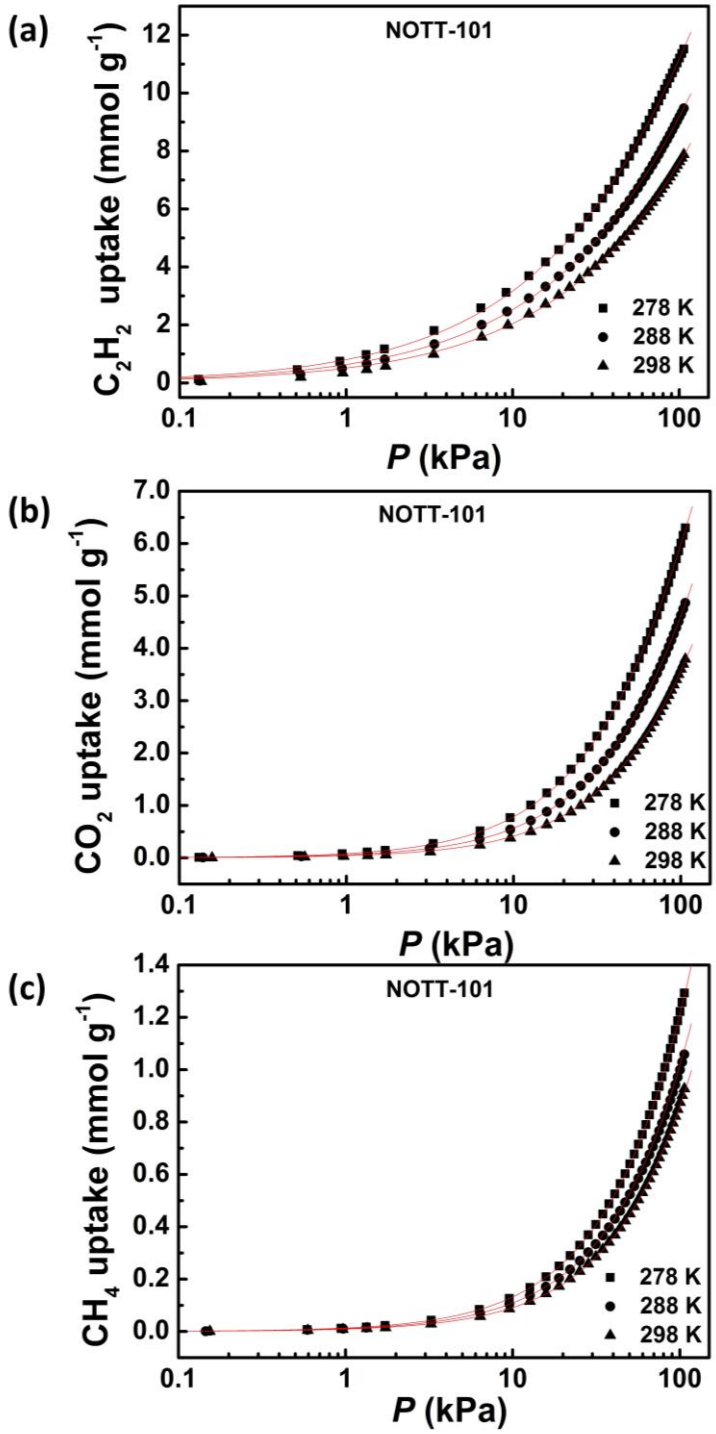

Fig. S17 Comparison of the pure-component isotherm data for (a) C_2H_2, (b) CO_2, and (c) CH_4 in **NOTT-101** with the fitted isotherms at 278 K, 288 K, and 298 K.

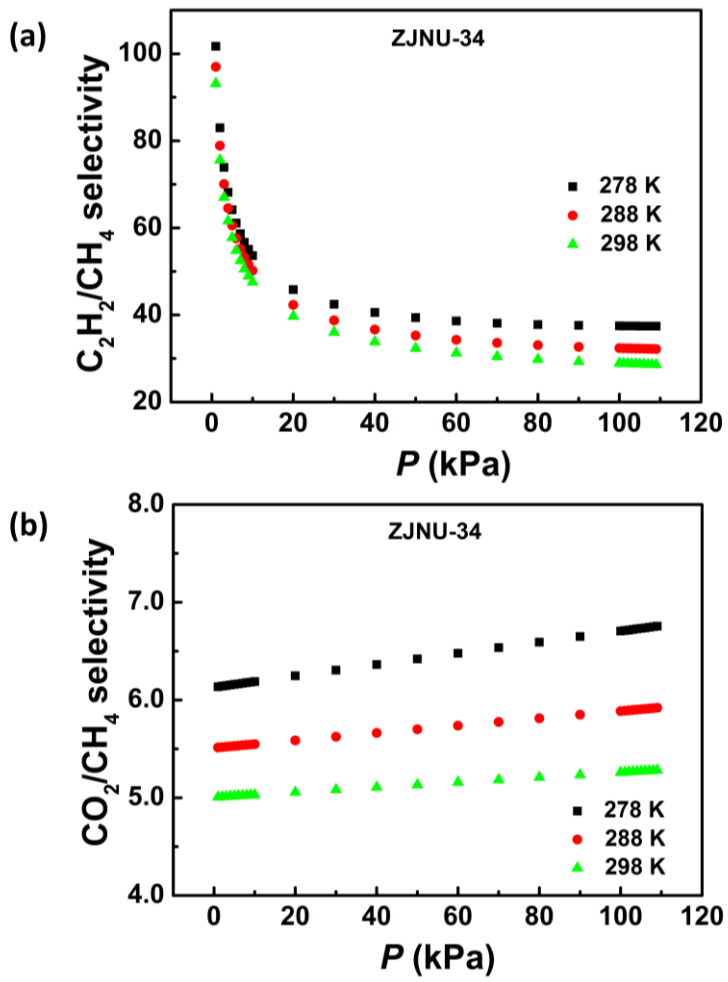

Fig. S18 IAST selectivities for the equimolar (a) C_2H_2/CH_4 and (b) CO_2/CH_4 gas mixtures in **ZJNU-34** at three different temperatures of 278 K, 288 K, and 298 K.

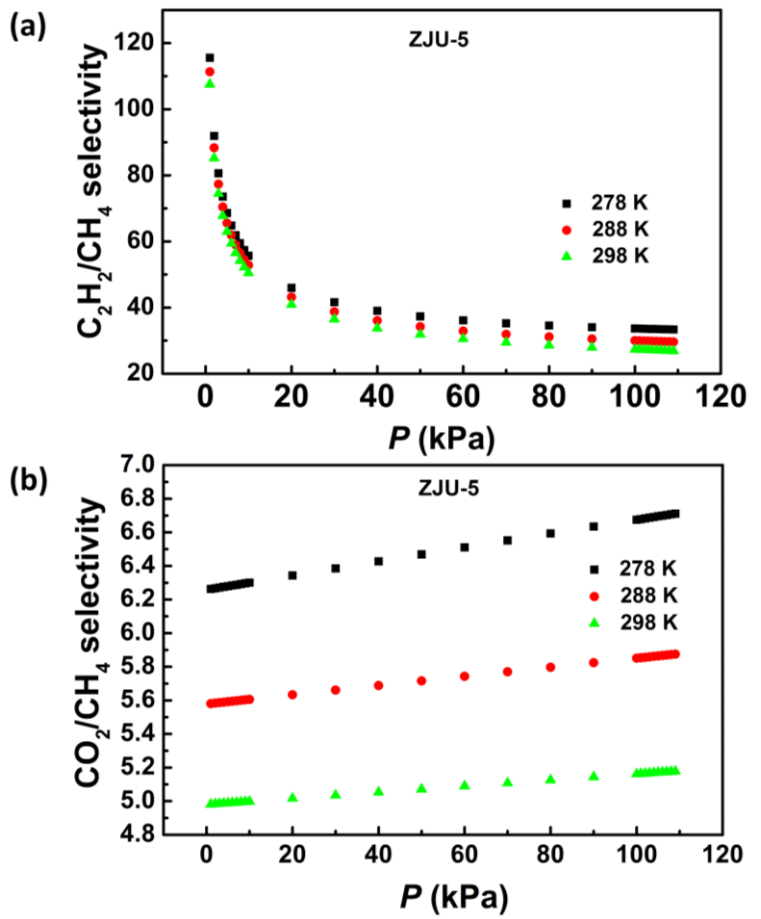

Fig. S19 IAST selectivities for the equimolar (a) C_2H_2/CH_4 and (b) CO_2/CH_4 gas mixtures in **ZJU-5** at three different temperatures of 278 K, 288 K, and 298 K.

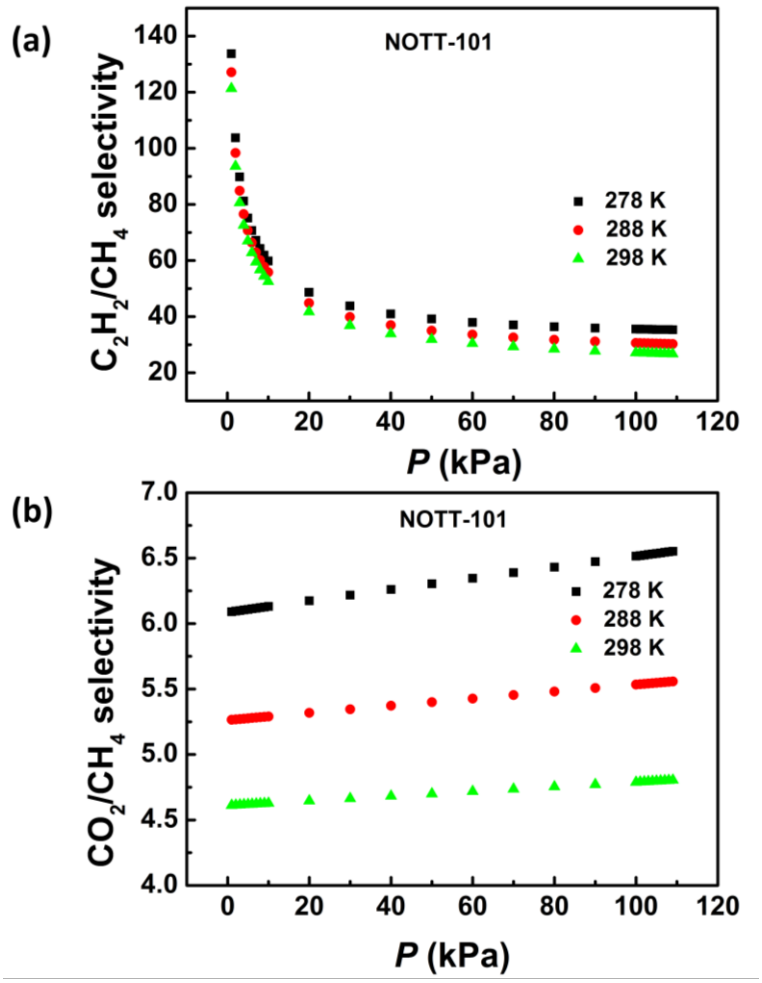

Fig. S20 IAST selectivities for the equimolar (a) C_2H_2/CH_4 and (b) CO_2/CH_4 gas mixtures in **NOTT-101** at three different temperatures of 278 K, 288 K, and 298 K.

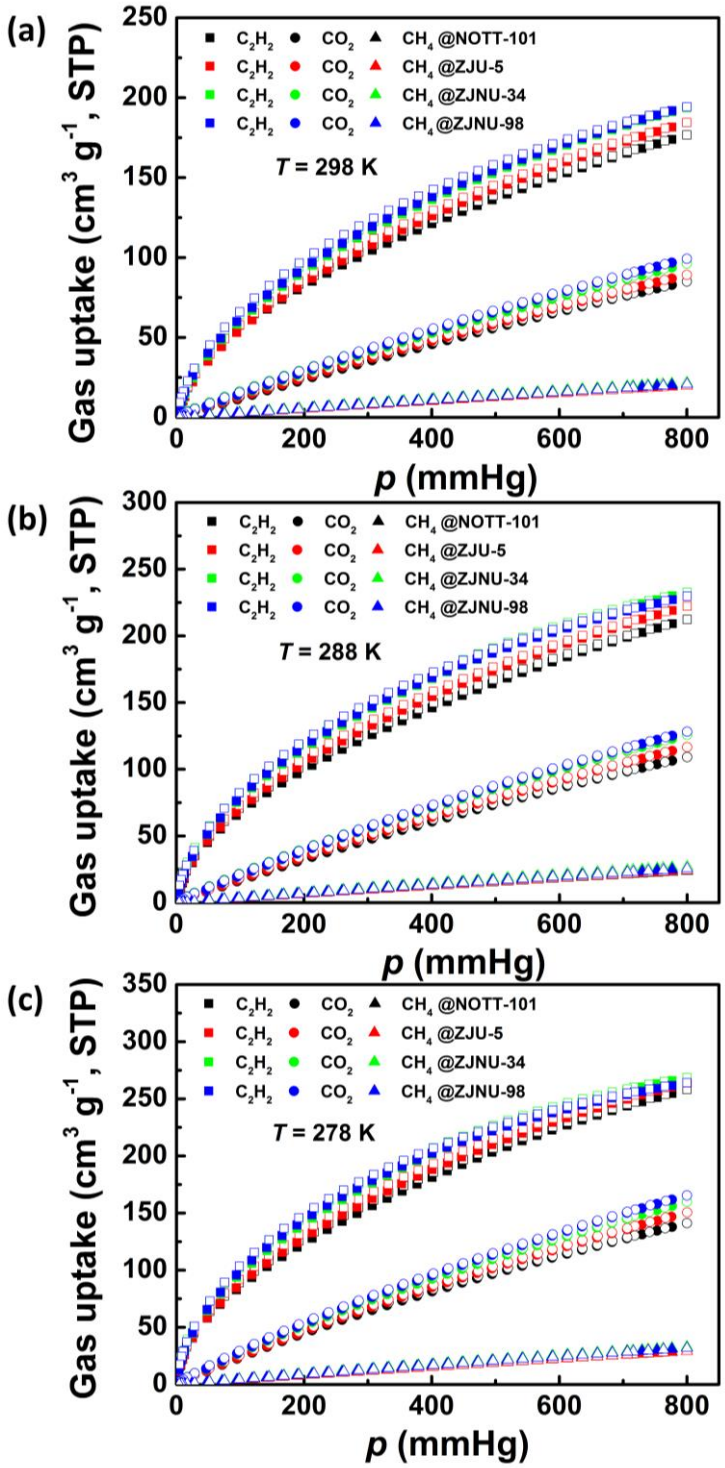

Fig. S21 Comparison of C_2H_2, CO_2 and CH_4 isotherms of **ZJNU-98**, ZJNU-34, ZJU-5 and NOTT-101 at three different temperatures of (a) 298 K, (b) 288 K and (c) 278 K. The solid and open symbols represent adsorption and desorption, respectively.

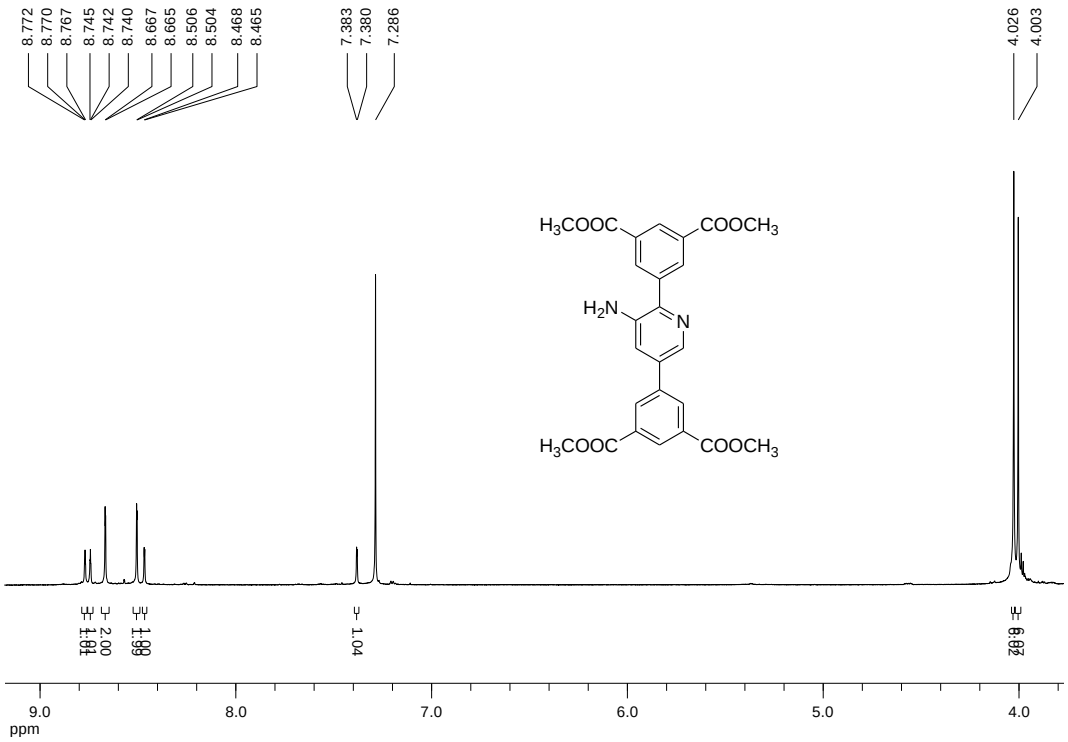
8.772
8.770
8.767
8.745
8.742
8.740
8.667
8.665
8.506
8.504
8.468
8.465
7.383
7.380
7.286
4.026
4.003
H3COOC
COOCH3
H2N
N
H3COOC
COOCH3
1.04
9.0
8.0
7.0
6.0
5.0
4.0
ppm

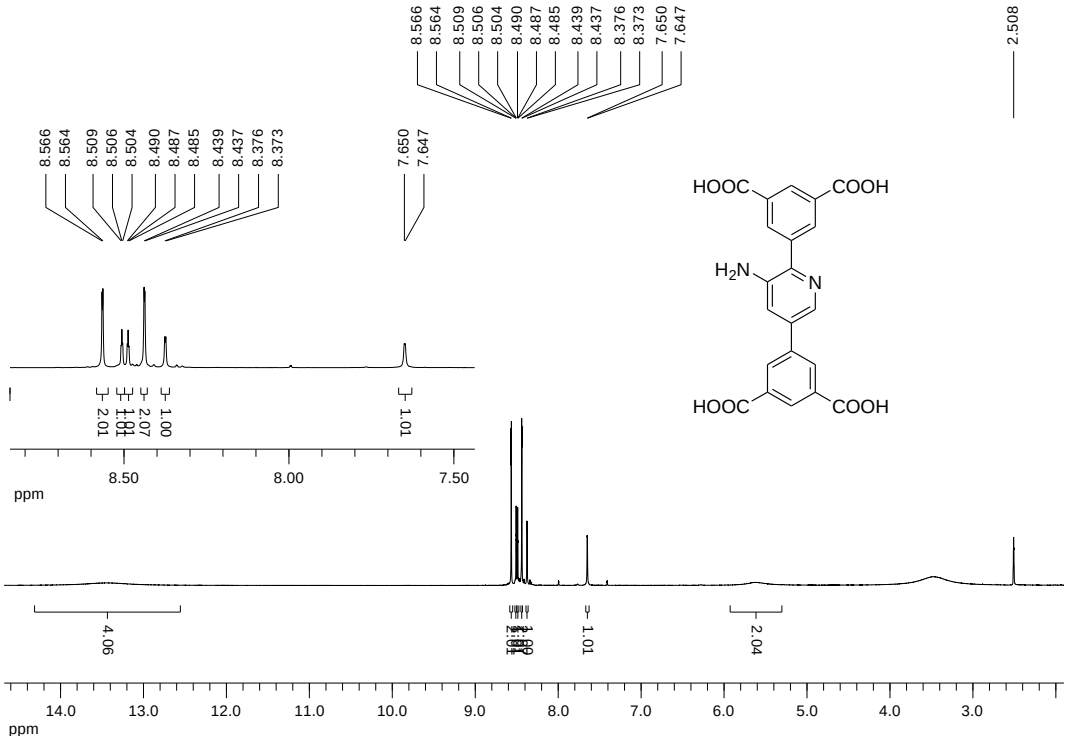
8.566
8.564
8.509
8.506
8.504
8.490
8.487
8.485
8.439
8.437
8.376
8.373
7.650
7.647
2.508
HOOC
COOH
H2N
N
HOOC
COOH
2.01
2.07
1.00
1.01
8.50
8.00
7.50
ppm
4.06
1.01
2.04
14.0
13.0
12.0
11.0
10.0
9.0
8.0
7.0
6.0
5.0
4.0
3.0
ppm

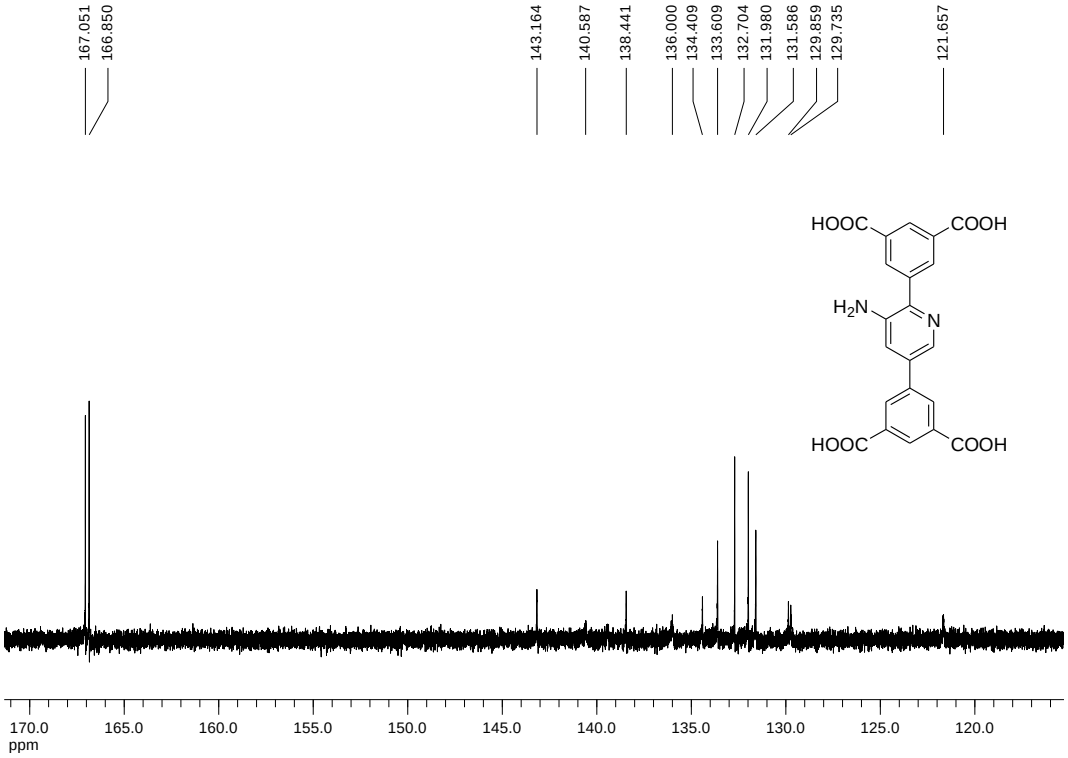

Fig. S22 ^{1}H and ^{13}C NMR spectra.

Table S1 Crystal data and structure refinement for **ZJNU-98**.

MOFs	**ZJNU-98**
Empirical formula	$C_{21}H_{14}Cu_2N_2O_{10}$
Formula weight	581.44
λ (Å)	0.71073
Crystal system	Trigonal
Space group	*R-3m*
Unit cell dimensions	a = 18.7125(10) Å b = 18.7125(10) Å c = 38.299(3) Å $\alpha = 90^o$ $\beta = 90^o$ $\gamma = 120^o$
V (Å^3)	11614.0(15)
Z	9
D_c (g cm^{-3})	0.747
μ (mm^{-1})	0.850
F(000)	2628
θ range for data collection (^{o})	2.177 to 27.402
Limiting indices	$-23 \leq h \leq 24$ $-22 \leq k \leq 24$ $-46 \leq l \leq 49$
Reflections collected / unique	34905 / 3199
R_{int}	0.0314
Max. and min. transmission	0.919 and 0.894
Refinement method	Full-matrix least-squares on F^2
Data/restraints/parameters	3199 / 0 / 106
Goodness-of-fit on F^2	0.865
Final R indices [$I > 2\sigma(I)$]	R_1 = 0.0443 wR_2 = 0.1694
R indices (all data)	R_1 = 0.0487 wR_2 = 0.1861
Largest diff. peak and hole (e·Å^{-3})	0.870 and -0.378
CCDC	1898821

Table S2 Langmuir-Freundlich parameters for adsorption of C_2H_2, CO_2, and CH_4 in **ZJNU-98**.

Guest	q_{sat} (mmol g^{-1})	b_0 $(kPa)^{-v}$	E (kJ mol^{-1})	v	R^2
C_2H_2	24.28222	1.07526×10^{-5}	18.791	0.70027	0.9998
CO_2	25.28245	2.25809×10^{-7}	22.507	1	0.99993
CH_4	13.4719	1.09446×10^{-6}	15.979	1	0.99999

Table S3 Langmuir-Freundlich parameters for adsorption of C_2H_2, CO_2, and CH_4 in ZJNU-34.

Guest	q_{sat} (mmol g^{-1})	b_0 $(kPa)^{-\nu}$	E (kJ mol^{-1})	ν
C_2H_2	27.75156	1.17624×10^{-5}	18.208	0.6891
CO_2	23.47517	2.52642×10^{-7}	22.378	1
CH_4	12.92465	1.42418×10^{-6}	15.577	1

Table S4 Langmuir-Freundlich parameters for adsorption of C_2H_2, CO_2, and CH_4 in ZJU-5.

Guest	q_{sat} (mmol g^{-1})	b_0 $(kPa)^{-v}$	E (kJ mol^{-1})	v	R^2
C_2H_2	40.70198	1.52745×10^{-5}	16.496	0.65541	0.99978
CO_2	26.88883	2.16142×10^{-7}	22.123	1	0.99991
CH_4	15.30125	1.81459×10^{-6}	14.268	1	0.99984

Table S5 Langmuir-Freundlich parameters for adsorption of C_2H_2, CO_2, and CH_4 in NOTT-101.

Guest	q_{sat} (mmol g^{-1})	b_0 $(kPa)^{-v}$	E (kJ mol^{-1})	v
C_2H_2	59.19957	1.48802×10^{-5}	15.787	0.61397
CO_2	22.75234	2.18689×10^{-7}	22.416	1
CH_4	13.39522	3.93239×10^{-6}	12.786	1

Table S6 Summary of gas adsorption properties of **ZJNU-98**, ZJNU-34, ZJU-5, and NOTT-101.

MOFs	S_{BET}/ $S_{Langmuir}$ ($m^2 g^{-1}$)	V_p ($cm^3 g^{-1}$)	D_c ($g\ cm^{-3}$)	C_2H_2 uptake[a] ($cm^3 g^{-1}$)			CO_2 uptake[a] ($cm^3 g^{-1}$)			CH_4 uptake[a]			C_2H_2/CH_4[a] IAST selectivity			CO_2/CH_4[a] IAST selectivity		
				298 K	288 K	278 K	298 K	288 K	278 K	298 K	288 K	278 K	298 K	288 K	278 K	298 K	288 K	278 K
NOTT-101	2772/2961	1.0579	0.6838	176.6	212.3	258.1	85.0	109.1	141.2	20.8	23.7	29.0	26.7	30.3	35.3	4.80	5.56	6.55
ZJU-5	2670/2922	1.0385	0.679	184.4	222.3	263.9	89.1	116.6	150.6	19.7	24.1	29.1	26.9	29.6	33.4	5.18	5.88	6.71
ZJNU-34	2459/2704	0.9687	0.7064	193.8	232.8	268.6	96.2	125.8	159.9	21.7	27.1	32.9	28.6	32.2	37.4	5.28	5.92	6.75
ZJNU-98	2378/2607	0.9324	0.7017	194.3	229.7	264.1	99.2	128.2	165.5	20.8	25.6	31.8	30.5	34.1	39.2	5.70	6.36	7.21

$S_{BET}/S_{Langmuir}$ = BET and Langmuir specific surface areas; V_p = experimental pore volume; D_c = calculated framework density without solvent molecules and the terminal water molecules; [a] at 1 atm

Table S7 Summary of selective C_2H_2/CH_4 and CO_2/CH_4 adsorption properties of some typical MOFs reported so far.

MOFs	S_{BET} (m^2 g^{-1})	C_2H_2 uptake[a] (cm^3 g^{-1})	CO_2 uptake[a] (cm^3 g^{-1})	C_2H_2/CH_4 selectivity[a]	CO_2/CH_4 selectivity[a]	*Ref.*
NKMOF-1-Ni	382	61.0	51.1	6409.1	NA	[1]
PMOF-3	1378	117.3	74.5	156.5	5.1	[2]
Ni-TIPA	404.6	56.8	39.0	112.2	NA	[3]
Cu-TDPAH	2171	155.7	116	82	18	[4]
Cu-TDPAT	1938	177.7	NA	82[b]	NA	[5]
UTSA-15	553	34	31	55.6[b]	24.2[b]	[6]
$Mn(INA)_2$	236	59.7	NA	51	NA	[7]
ZJNU-54	2134	211	120	45.0	6.1	[8]
ZJU-195	1721.9	214.2	105.0	43.4	NA	[9]
UTSA-57	206.5	32	37	43.1	20.0	[10]
FJI-Y3	952	118	NA	41.5	NA	[11]
FJI-C1	1726.3	93.8	41.2	39.3	5.89	[12]
UPC-21	1725.1	139.5	NA	38.1	NA	[13]
ZJNU-56	1655	189	122	35.7	7.0	[14]
M'MOF-20	42	21	10	34.9[b]	6.8[b]	[15]
MFM-130	2173	85.9	59	34.7[b]	NA	[16]
ZJNU-69	1655	171.7	104.1	34.5	7.14	[17]
ZJNU-93	1952	164.0	96.2	34.4	5.2	[18]
ZJNU-81	2720	184.2	99.0	32.4	5.46	[19]
ZJNU-59	2043	199.5	109.4	31.9	6.0	[20]
ZJNU-89	1618	181.3	103.0	30.7	5.8	[21]
ZJNU-82	2231	195.4	95.4	30.1	5.37	[19]
ZJNU-76	1996	179.2	95.8	29.7	5.43	[22]
ZJNU-88	1693	166.0	99.2	28.9	5.4	[21]
ZJNU-77	2432	120.2	78.1	28.6	5.7	[23]

ZJNU-78	1311	122.0	82.0	28.4	5.9	[23]
UTSA-5	462	59.8	38.4	28.4[b]	10.2[b]	[24]
ZJNU-75	2063	188.6	99.2	28.2	5.44	[22]
ZJNU-70	1748	184.5	115.5	28.0	6.71	[17]
ZJNU-71	1860	200.4	115.6	27.6	5.73	[17]
ZJNU-71	1860	200.4	115.6	27.6	5.73	[25]
ZJU-199	987	128	62.4	27.3	NA	[26]
ZJNU-83	2015	196.7	102.7	26.5	4.95	[19]
UTSA-72	173	27.8	21.7	26.5	9.3	[27]
ZJNU-58	2487	157.1	81.6	25.7	5.5	[20]
ZJNU-91	2404	172.5	94.8	25.0	4.92	[28]
ZJNU-74	2243	180.0	88.1	24.9	4.80	[22]
ZJNU-92	2845	155.1	79.2	24.5	4.85	[28]
BUT-35	358	71.6	NA	23.5[b]	NA	[29]
BUT-70B	695	87.1	31.3	23.3	NA	[30]
PCM-48	300	25.54	21	23.3	6.1	[31]
MFM-127	1557	208[c]	66.5	21.2[c]	3.33	[32]
UTSA-222	703	85.3	42.7	19	NA	[33]
UTSA-33	660	83.6	NA	18	NA	[34]
FJU-36	409.0	52.2	35.5	17.7	NA	[35]
$Zn_5(BTA)_6(TDA)_2$	414	44	37	15.5	9.1	[36]
UTSA-36	495	56.8	NA	13.8[b]	NA	[37]
QMOF-1	140	41.5	24.6	13.5	6.4	[38]
ZJU-30	228	52.6	NA	9.58[b]	NA	[39]
UPC-33	933.8	44.3	31.8	7.78	8.09	[40]
UTSA-10	1090	43.0	NA	6.2	NA	[41]
MFM-126	1004	124[c]	103.7	NA	11.7	[32]
SNNU-95	206.6	15.1	14.7	NA	NA	[42]

S_{BET} = BET specific surface area; [a] at ambient conditions; [b] adsorption selectivity based on Henry's Law constants; [c] 273 K, 1 bar; NA = not available

Reference

1. Y.-L. Peng, T. Pham, P. Li, T. Wang, Y. Chen, K.-J. Chen, K. A. Forrest, B. Space, P. Cheng, M. J. Zaworotko and Z. Zhang, *Angew. Chem. Int. Ed.*, 2018, **57**, 10971-10975.
2. O. Alduhaish, H. Wang, B. Li, T.-L. Hu, H. D. Arman, K. Alfooty and B. Chen, *ChemPlusChem*, 2016, **81**, 770-774.
3. H.-R. Fu, Y. Zhao, Z. Zhou, X.-G. Yang and L.-F. Ma, *Dalton Trans.*, 2018, **47**, 3725-3732.
4. K. Liu, B. Li, Y. Li, X. Li, F. Yang, G. Zeng, Y. Peng, Z. Zhang, G. Li, Z. Shi, S. Feng and D. Song, *Chem. Commun.*, 2014, **50**, 5031-5033.
5. K. Liu, D. Ma, B. Li, Y. Li, K. Yao, Z. Zhang, Y. Han and Z. Shi, *J. Mater. Chem. A*, 2014, **2**, 15823-15828.
6. Z. Chen, S. Xiang, H. D. Arman, J. U. Mondal, P. Li, D. Zhao and B. Chen, *Inorg. Chem.*, 2011, **50**, 3442-3446.
7. R.-G. Lin, L. Li, R.-B. Lin, H. Arman and B. Chen, *CrystEngComm*, 2017, DOI: 10.1039/C1037CE01766A.
8. J. Jiao, L. Dou, H. Liu, F. Chen, D. Bai, Y. Feng, S. Xiong, D.-L. Chen and Y. He, *Dalton Trans.*, 2016, **45**, 13373-13382.
9. L. Zhang, K. Jiang, Y. Li, D. Zhao, Y. Yang, Y. Cui, B. Chen and G. Qian, *Cryst. Growth Des.*, 2017, **17**, 2319-2322.
10. Z. Guo, D. Yan, H. Wang, D. Tesfagaber, X. Li, Y. Chen, W. Huang and B. Chen, *Inorg. Chem.*, 2015, **54**, 200-204.
11. Y.-X. Tan, Y. Si, W. Wang and D. Yuan, *J. Mater. Chem. A*, 2017, **5**, 23276-23282.
12. Y. Huang, Z. Lin, H. Fu, F. Wang, M. Shen, X. Wang and R. Cao, *ChemSusChem*, 2014, **7**, 2647-2653.
13. M. Zhang, X. Xin, Z. Xiao, R. Wang, L. Zhang and D. Sun, *J. Mater. Chem. A*, 2017, **5**, 1168-1175
14. J. Jiao, D. Jiang, F. Chen, D. Bai and Y. He, *Dalton Trans.*, 2017, **46**, 7813-7820.
15. Z. Zhang, S. Xiang, K. Hong, C. D. Madhab, H. D. Arman, M. Garcia, J. U. Mondal, K. M. Thomas and B. Chen, *Inorg. Chem.*, 2012, **51**, 4947-4953.
16. Y. Yan, M. Juríček, F.-X. Coudert, N. A. Vermeulen, S. Grunder, A. Dailly, W. Lewis, A. J. Blake, J. F. Stoddart and M. Schröder, *J. Am. Chem. Soc.*, 2016, **138**, 3371-3381.
17. F. Chen, Y. Wang, D. Bai, M. He, X. Gao and Y. He, *J. Mater. Chem. A*, 2018, **6**, 3471-3478.
18. S. Li, J. Wu, X. Gao, M. He, Y. Wang, X. Wang and Y. He, *CrystEngComm*, 2018, **20**, 7178-7183.
19. M. He, Y. Wang, X. Gao, S. Li and Y. He, *Dalton Trans.*, 2018, **47**, 8983-8991.
20. Y. Wang, M. He, X. Gao, S. Li, S.-s. Xiong, R. Krishna and Y. He, *ACS Appl. Mater. Interfaces*, 2018, **10**, 20559-20568.
21. Y. Wang, M. He, X. Gao, P. Long, Y. Zhang, H. Zhong, X. Wang and Y. He, *Dalton Trans.*, 2018, **47**, 12702-12710.
22. F. Chen, D. Bai, Y. Wang, D. Jiang and Y. He, *Mater. Chem. Front.*, 2017, **1**, 2283-2291.
23. F. Chen, D. Bai, Y. Wang, M. He, X. Gao and Y. He, *Dalton Trans.*, 2018, **47**, 716-725.
24. G. Chen, Z. Zhang, S. Xiang and B. Chen, *CrystEngComm*, 2013, **15**, 5232-5235.
25. F. Chen, D. Bai, D. Jiang, Y. Wang and Y. He, *Dalton Trans.*, 2017, **46**, 11469 -11478.

26. L. Zhang, C. Zou, M. Zhao, K. Jiang, R. Lin, Y. He, C.-D. Wu, Y. Cui, B. Chen and G. Qian, *Cryst. Growth Des.*, 2016, **16**, 7194-7197.
27. H. Alawisi, B. Li, Y. He, H. D. Arman, A. M. Asiri, H. Wang and B. Chen, *Cryst. Growth Des.*, 2014, **14**, 2522-2526.
28. Y. Wang, M. He, X. Gao, Y. Zhang, H. Zhong, P. Long, X. Wang and Y. He, *Inorg. Chem. Front.*, 2018, **5**, 2811-2817.
29. Y. Han, H. Zheng, K. Liu, H. Wang, H. Huang, L.-H. Xie, L. Wang and J.-R. Li, *ACS Appl. Mater. Interfaces*, 2016, **8**, 23331-23337.
30. Z.-J. Guo, J. Yu, Y.-Z. Zhang, J. Zhang, Y. Chen, Y. Wu, L.-H. Xie and J.-R. Li, *Inorg. Chem.*, 2017, **56**, 2188-2197.
31. J. E. R. III, K. M. Walsh, B. Li, P. Kunal, B. Chen and S. M. Humphrey, *Chem. Commun.*, 2018, **54**, 9937-9940.
32. J. D. Humby, O. Benson, G. L. Smith, S. P. Argent, I. d. Silva, Y. Cheng, S. Rudić, P. Manuel, M. D. Frogley, G. Cinque, L. K. Saunders, I. J. Vitórica-Yrezábal, G. F. S. Whitehead, T. L. Easun, W. Lewis, A. J. Blake, A. J. Ramirez-Cuesta, S. Yang and M. Schröder, *Chem. Sci.*, 2019, **10**, 1098-1106
33. J.-x. Ma, J. Guo, H. Wang, B. Li, T. Yang and B. Chen, *Inorg. Chem.*, 2017, DOI: 10.1021/acs.inorgchem.1027b00762.
34. Y. He, Z. Zhang, S. Xiang, F. R. Fronczek, R. Krishna and B. Chen, *Chem. Eur. J.*, 2012, **18**, 613-619.
35. L. Liu, Z. Yao, Y. Ye, L. Chen, Q. Lin, Y. Yang, Z. Zhang and S. Xiang, *Inorg. Chem.*, 2018, **57**, 12961-12968.
36. Z. Zhang, S. Xiang, Y.-S. Chen, S. M. Lee, T. Phely-Bobin and B. Chen, *Inorg. Chem.*, 2010, **49**, 8444-8448.
37. M. C. Das, H. Xu, S. Xiang, Z. Zhang, H. D. Arman, G. Qian and B. Chen, *Chem. Eur. J.*, 2011, **17**, 7817-7822.
38. R.-G. Lin, R.-B. Lin and B. Chen, *J. Solid State Chem.*, 2017, **252**, 138-141.
39. J. Cai, J. Yu, H. Xu, Y. He, X. Duan, Y. Cui, C. Wu, B. Chen and G. Qian, *Cryst. Growth Des.*, 2013, **13**, 2094-2097.
40. W. Fan, Y. Wang, Q. Zhang, A. Kirchon, Z. Xiao, L. Zhang, F. Dai, R. Wang and D. Sun, *Chem. Eur. J.*, 2017, **24**, 2137-2143.
41. Y. He, C. Song, Y. Ling, C. Wu, R. Krishna and B. Chen, *APL Mater.*, 2014, **2**, 124102.
42. H. Li, S. n. Li, X. Hou, Y. Jiang, M. Hua and Q.-G. Zhai, *Dalton Trans.*, 2018, **47**, 9310-9316.